Solid Earth
Discussions

# 1 Remote sensing data processing by multivariate regression analysis
# 2 method for iron mineral resource potential mapping: A case study in
# 3 Sarvian area, central Iran.

4 Edris Mansouri[1], Faranak Feizi[2*], Alireza Jafari Rad[3], Mehran Arian[4]

5

6 1- Department of Geology, Science and Research Branch, Islamic Azad University, Tehran, Iran

7 2- Department of Mining Engineering, South Tehran Branch, Islamic Azad University, Tehran, Iran

8 3- Department of Geology, Science and Research branch, Islamic Azad University, Tehran, Iran

9 4- Department of Geology, Science and Research Branch, Islamic Azad University, Tehran, Iran

10 *corresponding author

11 Fax number: +98 021 88830012; Cell: +98 912 3006753; faranakfeizi@gmail.com.

## 12 ABSTRACT

13 This paper used multivariate regression to create a mathematical model (with reasonable accuracy) for iron skarn

14 exploration in the region of the interest and generalizing multivariate regression in Mineral Prospectivity Mapping

15 (MPM) field. The main target of this manuscript is to exert multivariate regression analysis (as a MPM method) to

16 iron outcrops mapping from northeast part of the study area to discover new iron deposits in other parts. Two types of

17 multivariate regression models as two linear equations were employed to discover new mineral deposits. The Aster

18 satellite image bands (14 bands) sets as Unique Independent Variables (UIVs) and iron outcrops map as dependent

19 variables were used for MPM. According to the results of p-value, $R^2$ and $R_{adj}^2$, the second regression model (which

20 was a multiples and exponents of UIVs) was the fitted model versus other models. Also the accuracy of the model

21 was confirmed by iron outcrops map and geological observations. Based on field observation iron mineralization

22 occurs as contact of limestone and intrusive rocks (skarn type). Iron minerals consist dominantly of magnetite,

23 hematite and goethite.

24

25 **Key words:** Multivariate regression, Mineral Prospectivity Mapping, Iron, Sarvian

26

## 1. INTRODUCTION

Diagnosing futuristic zones and finding new mineral deposits in the region of interest, is the definitive main of mineral investigation. One way to achieve this aim is Using satellite image processing for identify Mineral Prospectivity Mapping (MPM) (Carranza, 2008; Abedi et al., 2013; Golshadi et al., 2016 and Feizi et al., 2012).

The utilization of satellite images for mineral investigation has been extremely effective in indicating out the attendance of minerals. Likewise, remote sensing gives the synoptic view, which is useful in distinguishing proof and delineation of different land frames, linear features, and structural elements (Feizi and Mansouri, 2013b).

The main objective of this manuscript is to use multivariate regression analysis (as a MPM method) to pixel values of Aster satellite image from north-east part of the study area to identify new iron deposits in other parts. Two types of multivariate regression models utilized to find new mineral deposits, using pixel values of Aster satellite image bands (14 band) sets as Unique Independent Variables (UIVs) and Iron outcrops surface (digitized by geology map of study area (scale 1:5000) and check field) data as dependent variables.

Regression analyses have been utilized as a part of numerous logical fields, such as geosciences.

Identification of stream sediment anomalies have been used by multiple regression analyses (e.g., Carranza, 2010a; Carranza, 2010b). Likewise, multivariate regression has been effectively utilized by Granian et al. (2015) to display subsurface mineralization from lithogeochemical information. Granian et al. (2015) utilized four types of multivariate regression models to depict significant surface geochemical anomalies for acknowledgment subsurface gold mineralization utilizing borehole data as dependent variables and surface lithogeochemical data as independent variables.

This paper utilized multivariate regression to make a mathematical model (with sensible precision) for iron potential zones investigation in the region of the interest and summing up multivariate regression in remote sensing field.

## 2. STUDY AREA

The Sarvian area is located in the Orumieh-Dokhtar magmatic arc in Central of Iran (Fig. 1a). This magmatic arc is the most imperative metallogenic area inside the district and hosts the majority of the larger metals deposits such as lead, zinc, copper and iron (Feizi et al., 2016 and Feizi et al., 2017).

The explored zone determined by Eocene intrusive rocks and carbonates of Qom formation. Several types of metal and non-metal mineral ore deposits have as of now been reported in the

62    study area. According to the 1:100,000 geological map of Kahak, the lithology of this part includes
63    cream limestone with intercalations of marls (Qom formation), dark green, andesitic-basaltic lava,
64    volcanic breccia, hyaloclastic limestone, green megaporphyritic andesitic-basaltic lava,
65    rhyodacitic domes, tonalite-quartzdiorite, microquartzdiorite-microquartzmonzo-diorite, granite-
66    granodiorite, alteration of light green, grey tuff, tuffaceous sandstone and shale with intercalation
67    of nummulitic sandy limestone and andesitic lava, grey limestone, orbitolina bearing, thick bedded
68    to massive (Aptian–Albian) (Feizi et al., 2016) (Fig. 1b).

69    In view of the current confirmations and furthermore contact of intrusive bodies with carbonate
70    rocks (Qom arrangement) and Iron outcrops  in the north-east of study area, Calcic iron skarn ore
71    (Sarvian mine) is located in the northeast of study area (Feizi et al., 2017) (Fig. 2).
72
73    **3. MULTIVARIATE REGRESSION**

74    Regression analyses is a good statistical manner for analysing relationships among variables
75    (Granian et al., 2015). This strategy can show the conduct of an event (a dependent variable) in
76    light of related variables (some independent variables). In regression analyses, if a dependent
77    variable called ($Y$) and independent variables called ($x_i$), the equation is:

78    $$Y = f(x_i). \qquad (1)$$

79    Y could be linear or non-linear function. Linear regression is used for modeling mineral
80    prospetivity in the Sarvian area. For linear regression Y is defined as follows:

81    $$Y = a_0 + a_1 x_1 + a_2 x_2 + \cdots + a_i x_i + \varepsilon, \quad i = 1,2,\ldots,n. \quad (2)$$

82

83    For this function, the constant factor is $a_0$ , the random error is $\varepsilon$ , and the regression
84    coefficients are $a_i$. If there were $n$ samples in a data set, for each sample $t$ variables were
85    measured. Thus, function (2) can be as follows:

86

87    $$Y_i = \hat{a}_0 + \hat{a}_1 X_{i1} + \hat{a}_2 X_{i2} + \cdots + \hat{a}_t X_{it} + \varepsilon_i i = 1,2,\ldots,n. \qquad (3)$$

88

89

90    Equation (3) can be re-written as a matrix. The linear function matrix is:

91    $$[Y] = [X][A] + [\varepsilon]. \qquad (4)$$

92

$$[Y] = \begin{bmatrix} Y_1 \\ Y_2 \\ \cdot \\ \vdots \\ Y_n \end{bmatrix}; \; [A] = \begin{bmatrix} \hat{a}_0 \\ \hat{a}_1 \\ \cdot \\ \vdots \\ \hat{a}_t \end{bmatrix}; \; [X] = \begin{bmatrix} 1 & X_{11} X_{12} \ldots X_{1t} \\ 1 & X_{21} X_{22} \ldots X_{2t} \\ & \cdot \\ & \vdots \\ 1 & X_{n1} X_{n2} \ldots X_{nt} \end{bmatrix}; \; [\varepsilon] = \begin{bmatrix} \varepsilon_1 \\ \epsilon_2 \\ \cdot \\ \vdots \\ \epsilon_n \end{bmatrix}. \quad (5)$$

93

94

95　　The least squares technique is used for estimating $[A]$ as the coefficient matrix, as follows:

96

97
$$[A] = [\textstyle\sum \,]^{-1}[C] = ([X]'[X])^{-1}[X]'[Y]. \quad (6)$$

98

99　　The inverse of variance-covariance samples matrix is $[\sum \,]^{-1}$ and the covariance matrix among
100　independent variable and samples is $[C]$. Thus by equation 6, the regression coefficients model is
101　calculated.

102　　In regression analysis, some criteria are required to review. These criteria are as follows:

103　　1. The variance and the mean of the random error should be a constant value and zero,
104　respectively.

105　　2. The coefficient of determination value ($R^2$) should be examined. This value is calculated as
106　follows (Granian et al., 2015):

107

108
$$R^2 = \frac{\sum_{i=1}^{n}(\hat{Y}_i - \bar{Y})^2}{\sum_{i=1}^{n}(Y_i - \bar{Y})^2} = 1 - \frac{\sum_{i=1}^{n}(Y_i - \hat{Y}_i)^2}{\sum_{i=1}^{n}(Y_i - \bar{Y})^2}. \quad (7)$$

109

110　　The mean of the variable ($\bar{Y}$), value of $i$th sample ($Y_i$) and estimated value of the $i$th sample
111　($\hat{Y}_i$) for dependent variables were used in equation 7. The calculated $R^2$ value determined within
112　[0, 1] range. The value of $R^2$ is close to 1 for well fitted models.

113　　1. According to the fact that adding independent variables to the model will increasing $R^2$
114　　　　value, the adjusted determination coefficient ($R^2_{adj}$) is defined as follows (Granian et al.,
115　　　　2015):

116
$$R^2_{adjusted} = 1 - \frac{n-1}{n-t}(1 - R^2). \quad (8)$$

117    As it was mentioned, $n$ is number of samples (or data) and $t$ is the number of variables (or
118    regression coefficients). If a set of explanatory variables are introduced into a regression one at a
119    time, with the $R^2_{adj}$ computed each time, the level at which $R^2_{adj}$ reaches a maximum, and decreases
120    afterward, would be a well fitted model.

121    2.    In regression analyses, the model should be fitted to the data. Accordingly, the p-value of
122          the regression model in Analysis of variance (ANOVA) test should be acceptable (less
123          than or equal to 0.05). Also calculating p-value of final coefficients for each model, could
124          help on optimizing and improving the model. This criterion could be considered after
125          choosing the best model.

126    4. **GEO-DATA SETS PREPARATION**

127    The iron ore skarn type located in the northeastern of Sarvian area. There are several iron vein
128    and outcrop in this area. According to the regional geological conditions of the area, the data set
129    of this iron mine is a good model for exploring the surrounding area. In this paper, satellite imagery
130    and map the geology of the mine is used as a training area. In the training area, this method can
131    model the iron outcrops (a dependent variable) based on Aster satellite image bands (some
132    independent variables) (Fig. 3).

133    **Figure 3 is about here.**

134    **4.1. REMOTE SENSING DATA (INDEPENDEBT VARIABLES)**

135    The ASTER sensor was propelled in December 1999 on board the Earth Observation System
136    (EOS) US Terra satellite to record sun powered radiation in 14 spectral bands (Table 1). ASTER
137    provides high-resolution images of the land surface, water, ice, and clouds using three separate
138    sensor subsystems covering 14 multi-spectral bands from visible to thermal infrared. The
139    significant resolution scales are 15m, 30m, and 90m in the visible, short-wave IR, and thermal fR,
140    respectively. ASTER consists of three different subsystems; the Visible and Near Infrared (VNIR),
141    the Shortwave Infrared (SWIR), and the Thermal Infrared (TIR). To find out more about each
142    module click on the item of interest (Feizi and Mansouri, 2013b and Mansouri and Feizi, 2016).

143    Several factors influence the signal measured at the sensor, for example, float of the sensor
144    radiometric calibration, atmospheric and topographical effects. In this way, Aster data collection
145    was utilized and radiance correlation, such as wavelength, dark subtract and log residual by
146    ENVI5.1 software which is basic for multispectral images, were utilized (Mansouri et al., 2015).

147    In this study after the corrections, pixles size of SWIR and TIR bands based on VNIR3 band
148    (Panchromatic band) convert to 15 meter, than use layer stacking function to build a new multiband
149    file from georeferenced images of various pixel sizes, extents, and projections.

150    **4.2. MAPPING OF IRON OUPCROPS (DEPENDENT VARIABLE)**

151    The iron ore skarn type located in the northeastern of Sarvian area. There are several iron vein
152 and outcrop in this area. In order to mapping of iron outcrops in the training area used from
153 Geological map (1:1000 scale) of iron ore deposit and check field. For preparing of this layer, the
154 shape file layer of iron outcrops convert to raster file with pixel size of 15 meter.

155    **5. REGRESSION ANALYSES IN THE STUDY AREA**

156    Regression analyses needs making proper models. Utilizing multiple, factorial, polynomial and
157 reaction surface regressions have been utilized as a part of numerous logical fields such as
158 geosciences (e.g. Granian et al., 2015). Thus, in this study; Model 1 ($Y_1$) was generated as a
159 multiple linear regression model and Model 2 ($Y_2$) was created from $Y_1$ plus multiplied UIVs. The
160 formulas of two mentioned models are presented in Table 2. So in summary, two linear equations
161 ($Y_1$ and $Y_2$) were utilized to discover new mineral deposits, using pixel values of Aster satellite
162 image as independent variables and map of iron outcrops as dependent variables. The models
163 which were proposed in this paper, had become more complexes respectively 1 to 2, model 2 has
164 106 coefficients (14 for UIVs, 1 as constant, 91 for multiples of UIVs) and model 1 has 15
165 coefficients (14 for UIVs, 1 as constant, 0 for multiples and exponents of UIVs) (Table 2).
166    For assessing the models which are exhibited in Table 2, regression analyses were performed
167 and the critical criteria which are mentioned before, were examined. The values of the $R^2$, $R^2_{adj}$
168 and p-value of ANOVA test of 2 multivariate regression models are provided in Table 3.
169

170    Also, Table 4 is presented the calculated coefficients of independent variables in regression
171 models. Other independent variables which are not mentioned in Table 4 were excluded variables.
172 The excluded variables have no effect on the models. This means that, excluded variables didn't
173 have any effect on iron mineralization and behavior of iron outcrop map.

174

175 6. **DISCUSSION**

176    For distinguishing the best model among 2 models, a few criteria are required to review.

177    Firstly, the variance and the mean of the random error were acceptable for all of regression
178 models. Secondly, based on Table 4, the p-values of ANOVA test of 2 multivariate regression
179 models were equal to 0. For regression models the acceptable p-value should be less than or equal
180 to 0.05. Thus, this criterion confirmed the validity of models without specifying the most
181 appropriate model.

182    On the other hand, the value of $R^2$ is close to 1 for well fitted models. The $R^2$ values of
183 regression models are presented in Table 3. The lowest $R^2$ belongs to $Y_1$ and the highest belongs to
184 $Y_2$. Thus, $Y_2$ model is better from $Y_1$ model.

Solid Earth
Discussions

Open Access

EGU

185   According to the fact that adding independent variables to the model will increasing $R^2$ value,
186   the $R^2_{adj}$ value should be checked. The $R^2_{adj}$ values of regression models are presented in Table 3.
187   As it was mentioned before, if a set of variables are introduced into a regression, with the
188   $R^2_{adj}$ computed each time, the level at which $R^2_{adj}$ reaches a maximum, and decreases afterward,
189   would be a well fitted model. So, according to Table 3, $Y_2$ would be the fitted model versus other
190   models. Thus, $Y_4$ regression model is the most appropriate model for Mineral Prospectivity
191   Mapping.

192   Thus according to the results of p-value (ANOVA test), $R^2$  and $R^2_{adj}$, the Second regression
193   model ($Y_2$) would be the fitted model versus other models. For generating the mineral prospectivity
194   map the formula of $Y_2$ was performed in ArcGIS software by raster calculator tool. The normalized
195   mineral prospectivity map of the study area is presented in Fig. 4.

196   To assess the exactness of the selected model, the created prospectivity map was checked by
197   the iron outcrops map in the northeast part of the study area (Fig. 5).  The locations of iron outcrops
198   have appropriate adoption with favorable areas of mineral prospectivity map. In addition the
199   adaption of prospectivity map with the iron outcrops in the northeast part of the study area, three
200   target areas with very high favourability, were checked and the prospectivity map was confirmed
201   by geological observations (Fig. 6). Based on field observation iron mineralization occurs as
202   contact of limestone and intrusive rocks (skarn type). Iron mineralizations consist dominantly of
203   magnetite, hematite and goethite. Therefore, the accuracy of mineral prospectivity map confirmed
204   in the Sarvian area.

205

206   **7. CONCLUSION**
207

208   The conclusions of this manuscript are presented in summary as follows.

209   1) The application of multivariate regression analysis (as a MPM method) was confirmed in
210   the Sarvian area. This paper used multivariate regression to create a mathematical model (with
211   reasonable accuracy) for iron mineral exploration in the region of the interest and generalizing
212   multivariate regression in MPM field.

213   2) Two types of multivariate regression models as two linear equations were employed to
214   discover new mineral deposits. According to the results of p-value, $R^2$ and $R^2_{adj}$, the second
215   regression model was the fitted model versus other models.

216   3) Also the accuracy of the model was confirmed by iron outcrops map and geological
217   observations. Based on field observation iron mineralization occurs contact of limestone and
218   intrusive rocks (skarn type). Iron mineralizations consist dominantly of magnetite, hematite and
219   goethite.

Solid Earth

Open Access

Discussions

EGU

224     **REFRENCES**

225     Carranza, E.J.M., 2008, Geochemical anomaly and mineral prospectivity mapping in GIS,
226     Handbook of Exploration Environmental Geochemistry. Elsevier, Amsterdam, 368 p.

227     Carranza, E.J.M., 2010a, Catchment basin modelling of stream sediment anomalies revisited:
228     incorporation of EDA and fractal analysis. Geochemistry: Exploration, Environment, Analysis,
229     10, 365–381.

230     Carranza, E.J.M., 2010b, Mapping of anomalies in continuous and discrete fields of stream
231     sediment geochemical landscapes. Geochemistry: Exploration, Environment, Analysis, 10, 171–
232     187.

233     Feizi, F. and Mansouri, E., 2012, Identification of Alteration Zones with Using ASTER Data
234     in A Part of Qom Province, Central Iran. Journal of Basic and Applied Scientific Research, 2, 73–
235     84.

236     Feizi, F. and Mansouri, E., 2013a, Separation of Alteration Zones on ASTER Data and
237     Integration with Drainage Geochemical Maps in Soltanieh, Northern Iran. Open Journal of
238     Geology, 3, 134–142.

239     Feizi, F. and Mansouri, E., 2013b, Introducing the Iron Potential Zones Using Remote Sensing
240     Studies in South of Qom Province, Iran. Open Journal of Geology, 3, 278–286.

241     Feizi, F., Mansouri, E. and KarbalaeiRamezanali, A., 2016, Prospecting of Au by Remote
242     Sensing and Geochemical Data Processing Using Fractal Modelling in Shishe-Botagh, Area (NW
243     Iran). Journal of the Indian Society of Remote Sensing, 44, 539–552.

244     Feizi, F., KarbalaeiRamezanali, A. and Mansouri, E., 2017, Calcic iron skarn prospectivity
245     mapping based on fuzzy AHP method, a case Study in Varan area, Markazi province,
246     Iran. Geosciences Journal, 21, 123–136.

247     Granian, H., Tabatabaei, S. H., Asadi, H. H. and Carranza, E. J. M., 2015, Multivariate
248     regression analysis of lithogeochemical data to model subsurface mineralization: a case study from
249     the Sari Gunay epithermal gold deposit, NW Iran. Journal of Geochemical Exploration, 148, 249–
250     258.

251    Golshadi, Z., KarbalaeiRamezanali, A. and Kafaei, K., 2016, Interpretation of magnetic data
252    in the Chenar-e Olya area of Asadabad, Hamedan, Iran, using analytic signal, Euler deconvolution,
253    horizontal gradient and tilt derivative methods. Bollettino di Geofisica Teorica ed Applicata, 57,
254    329–342.

255    Mansouri, E., Feizi, F. and KarbalaeiRamezanali, A., 2015, Identification of magnetic
256    anomalies based on ground magnetic data analysis using multifractal modelling: a case study in
257    Qoja-Kandi, East Azerbaijan Province, Iran. Nonlinear Processes in Geophysics, 22, 579–587.

258    Mansouri, E., Feizi, F., 2016, Introducing Au potential areas, using remote  sensing and
259    geochemical data processing using fractal method in Chartagh, western Azarbijan – Iran, E.
260    Mansouri,  F.  Feizi, Arch. Min. Sci., Vol., No 2, 397–414.

261

262

263

264

265

266

267

268

269

270

271

272

273

274

275

276

277

278

279     **Table 1.** Wavelength ranges and spatial resolutions of ASTER bands (Abrams, 2000).

280

| Module | VNIR | SWIR | TIR |
|---|---|---|---|
| Spectral bandwidth (μm) | Band 1 0.52 - 0.60 | Band 4 1.650 - 1.700 | Band 10 8.125 - 8.475 |
| | Band 2 0.63 - 0.69 | Band 5 2.145 - 2.185 | Band 11 8.475 - 8.825 |
| | Band 3 N 0.78 - 0.86 | Band 6 2.185 - 2.225 | Band 12 8.925 - 9.275 |
| | Band 3 B 0.78 - 0.86 (backward looking) | Band 7 2.235 - 2.285 | Band 13 10.25 - 10.95 |
| | | Band 8 2.295 - 2.395 | Band 14 10.95 - 11.65 |
| | | Band 9 2.360 - 2.430 | |
| Spatial resolution (m) | 15 | 30 | 90 |

281

282

283     **Table2.** Formula of regression models used for Aster satellite image bands

284

| Types of Regression | Number of coefficients | Formula |
|---|---|---|
| First-Degree | 15 | $Y_1 = a_0 + a_1 x_1 + a_2 x_2 + \cdots + a_{14} x_{14}$ |
| First-Degree | 106 | $Y_2 = Y_1 + a_{15} x_1 x_2 + a_{16} x_1 x_3 + \cdots + a_{27} x_1 x_{14} + a_{28} x_2 x_3 + a_{29} x_2 x_4 + \cdots$ $+ a_{39} x_2 x_{14} + a_{40} x_3 x_4 + a_{41} x_3 x_5 + \cdots + a_{50} x_3 x_{14}$ $+ a_{51} x_4 x_5 + \cdots + a_{60} x_4 x_{14} + a_{61} x_5 x_6 + \cdots + a_{69} x_5 x_{14}$ $+ a_{70} x_6 x_7 + \cdots + a_{77} x_6 x_{14} + a_{78} x_7 x_8 + \cdots + a_{84} x_7 x_{14}$ $+ a_{85} x_8 x_9 + \cdots + a_{90} x_8 x_{14} + a_{91} x_9 x_{10} + \cdots + a_{96} x_9 x_{14}$ $+ a_{97} x_{10} x_{11} + \cdots + a_{100} x_{10} x_{14}$ $+ a_{101} x_{11} x_{12} + \cdots + a_{103} x_{11} x_{14} + a_{104} x_{12} x_{13} + a_{105} x_{12} x_{14}$ $+ a_{106} x_{13} x_{14}$ |

285

286

287     **Table 3.** The values of the $R^2$ , $R^2_{adj}$ and p-value of ANOVA test of 2 multivariate regression

288     models

| Models | $R^2$ | $R^2_{adj}$ | p-value (ANOVA) |
|---|---|---|---|
| $Y_1$ | 0.738 | 0.715 | 0 |
| $Y_2$ | 0.847 | 0.829 | 0 |

289

290

291    **Table 4.** The calculated coefficients of regression models 1 and 2.

| Model 1 | | Model 2 | |
|---|---|---|---|
| **variables** | Coefficients ($a_i$) | variables | Coefficients ($a_i$) |
| **CST** | 0.275 | CST | 0.677 |
| $x_1$ | -0.01 | $x_1$ | -0.014 |
| $x_2$ | -0.12 | $x_2$ | -0.019 |
| $x_3$ | -0.019 | $x_3$ | -0.045 |
| $x_4$ | 0.003 | $x_4$ | 0.022 |
| $x_5$ | -0.006 | $x_5$ | -0.017 |
| $x_6$ | -0.005 | $x_6$ | -0.001 |
| $x_7$ | - | $x_7$ | - |
| $x_8$ | -0.004 | $x_8$ | -0.02 |
| $x_9$ | -0.005 | $x_9$ | -0.006 |
| $x_{10}$ | 0.009 | $x_{10}$ | -0.014 |
| $x_{11}$ | 0.005 | $x_{11}$ | 0.024 |
| $x_{12}$ | 0.016 | $x_{12}$ | 0.024 |
| $x_{13}$ | 0.002 | $x_{13}$ | 0.018 |
| $x_{14}$ | 0.022 | $x_{14}$ | 0.036 |
| - | - | $x_1 x_4$ | -0.0009 |
| - | - | $x_1 x_6$ | -0.0002 |
| - | - | $x_4 x_9$ | -0.0009 |
| - | - | $x_7 x_8$ | 0.00082 |

292

293
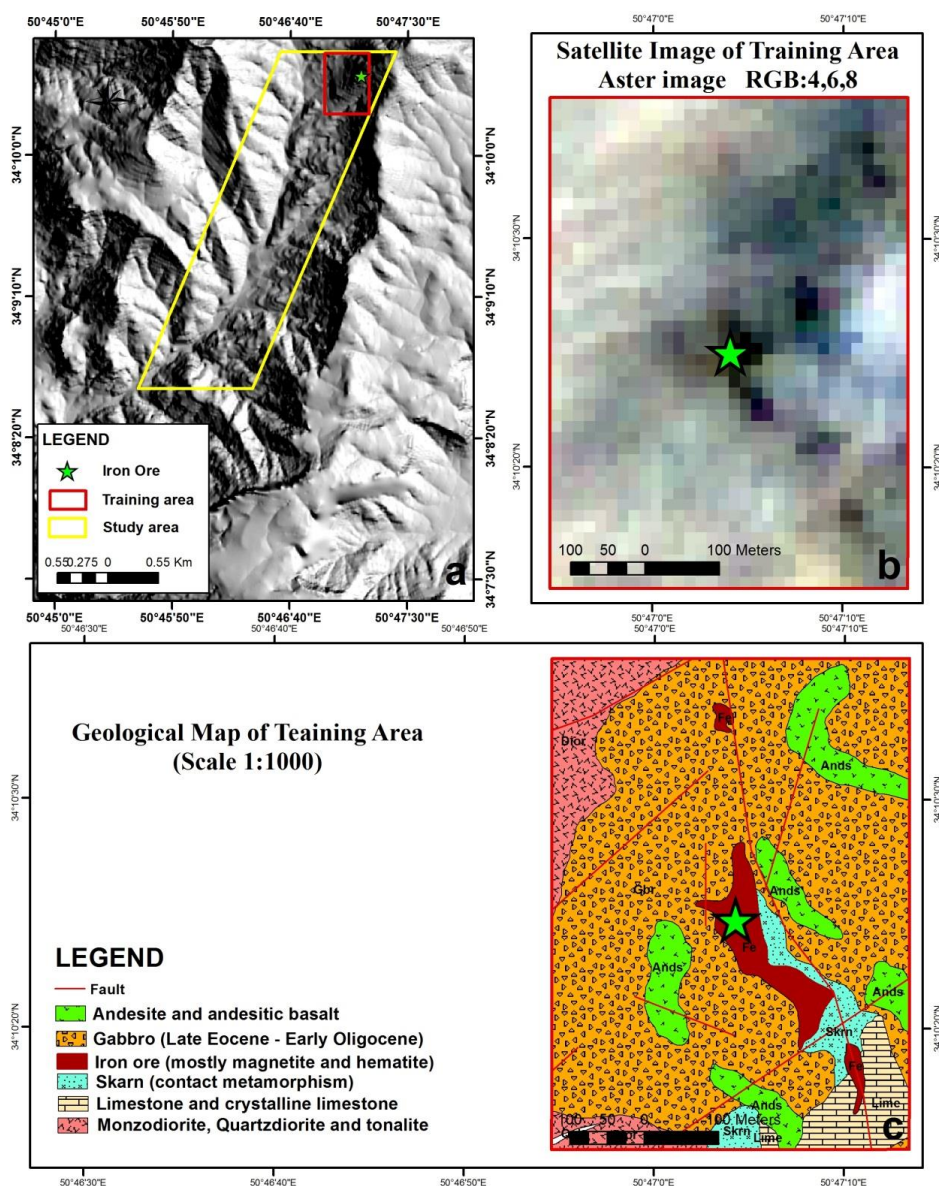
294
295
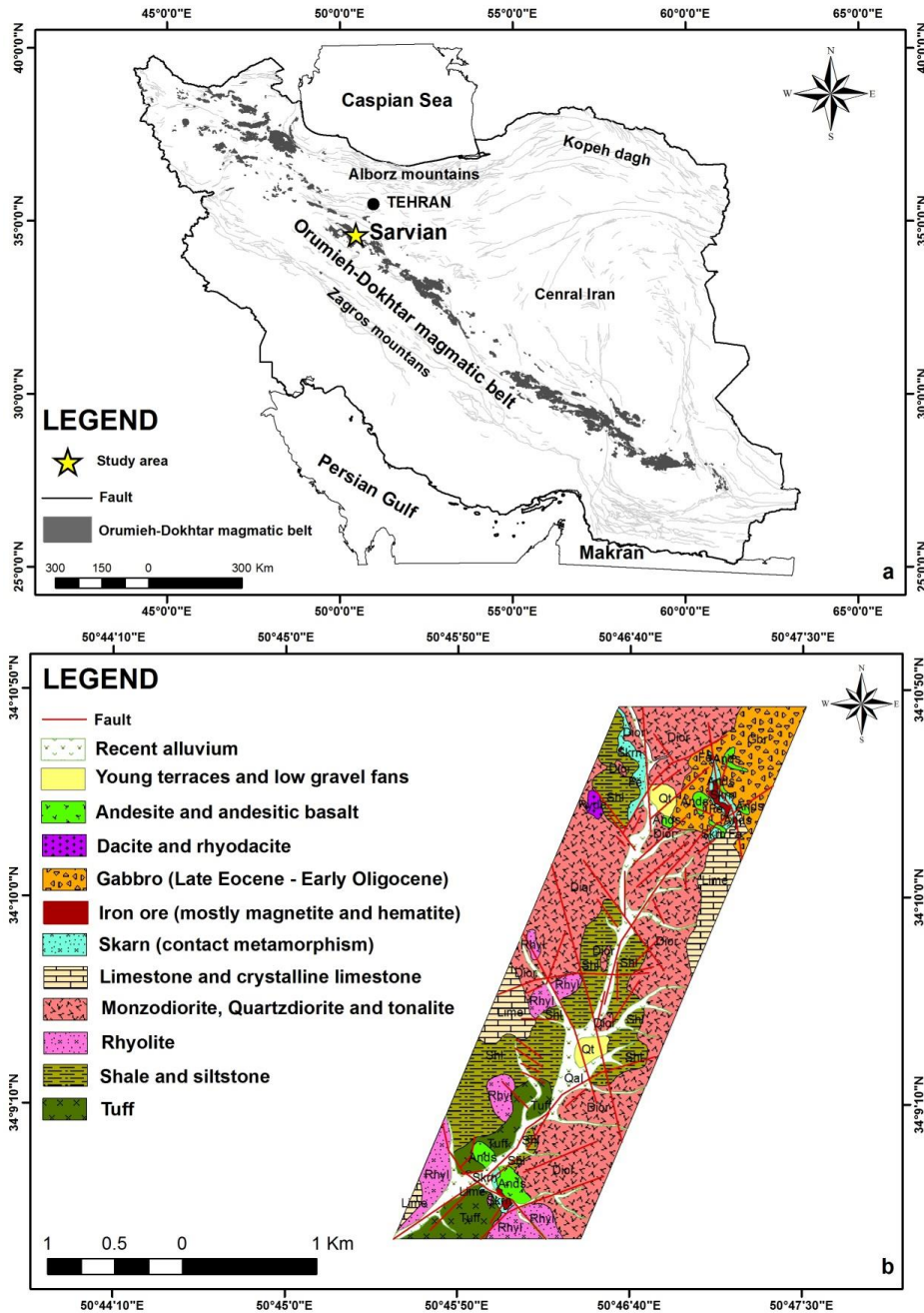
**Fig. 1. a)** The location of the Sarvian area in the Urumieh–Dokhtar magmatic belt, Iran **b)** Geological map
of Sarvian area (scale 1:25000)
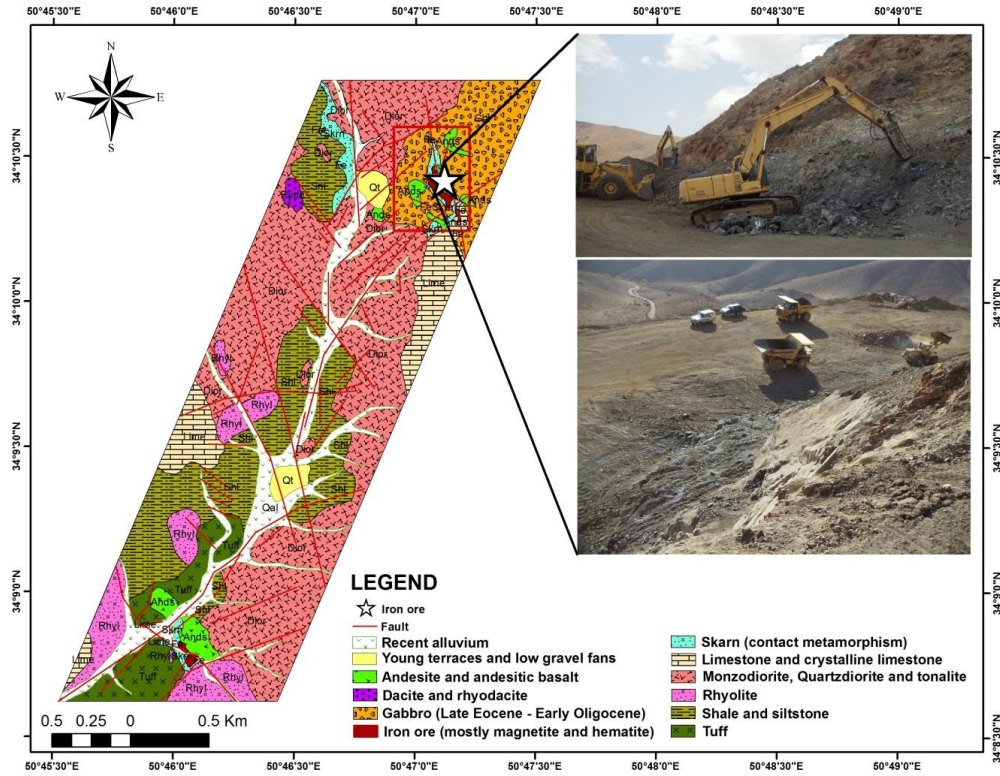
298

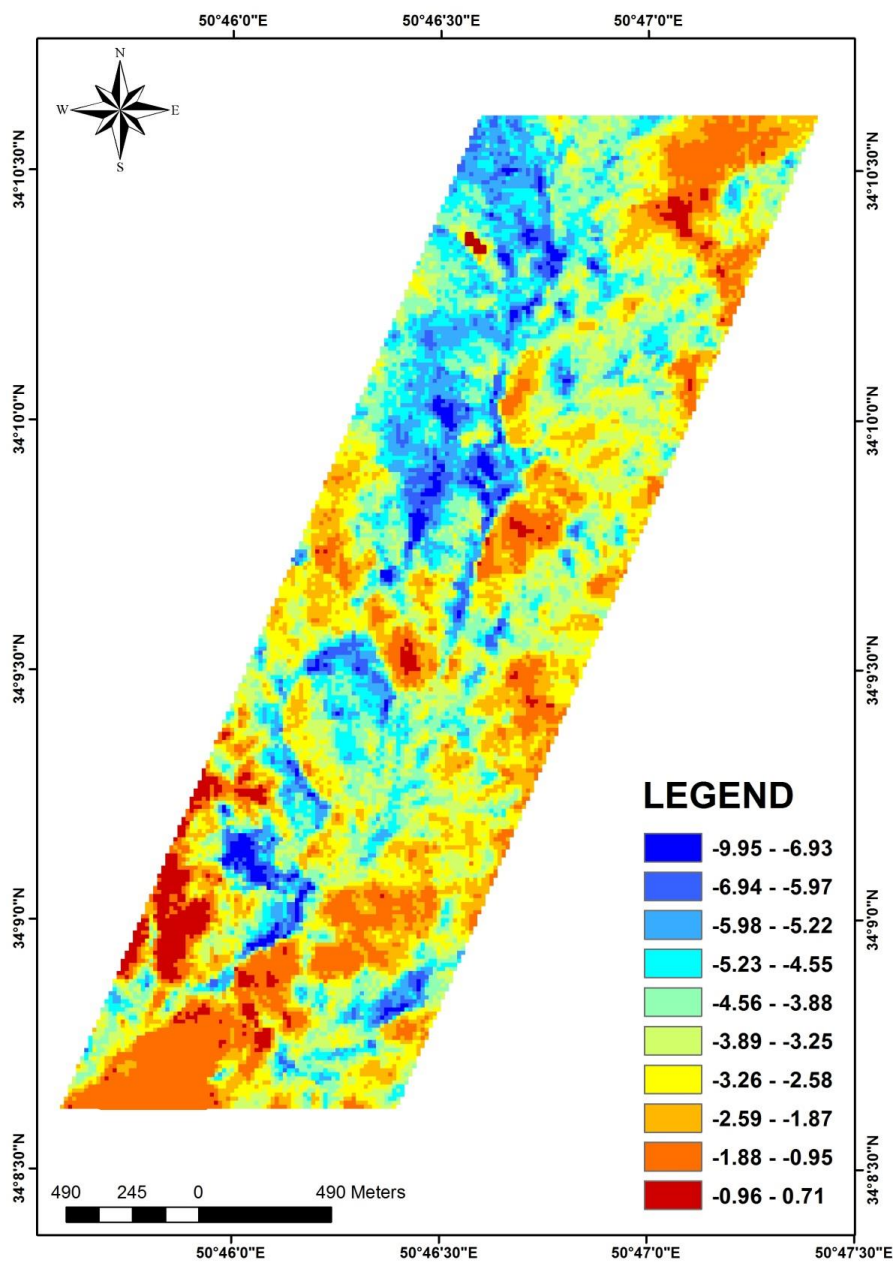299     **Fig. 2.** Location of Sarvian iron mine in the study area

300

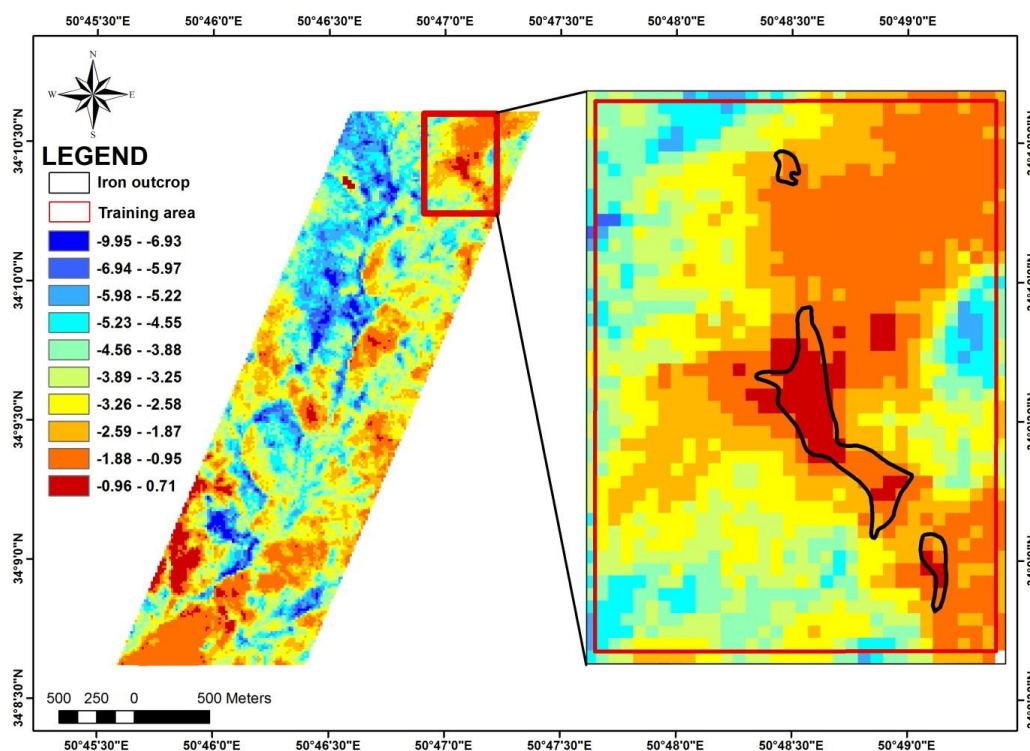**Fig. 3.** a) Location of training area in the study area. b) Aster satellite image in the training area

(RGB:4,6,8). c) Geological map (scale 1:1000) of training area.

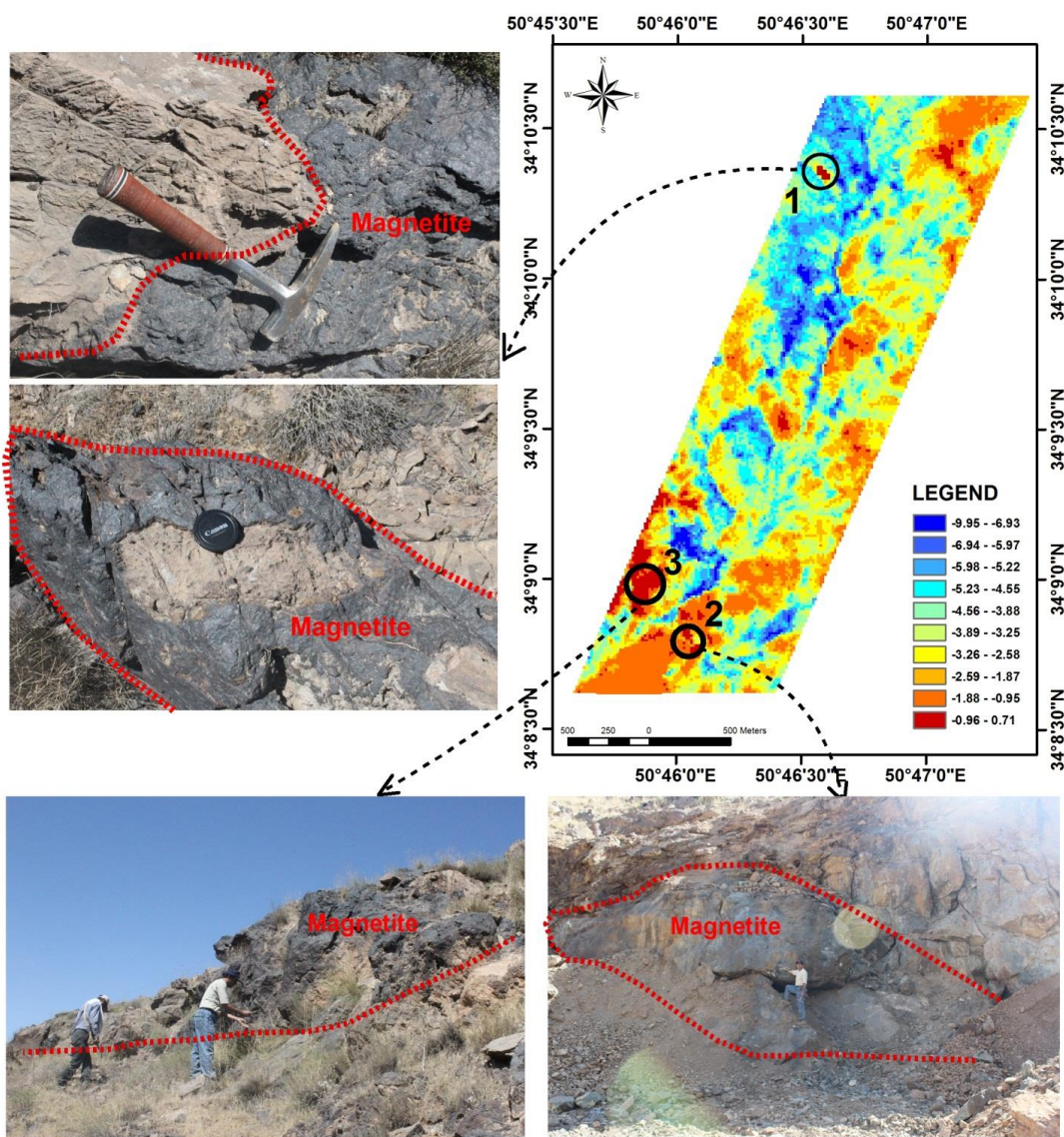**Fig. 4.** Mineral prospectivity map of the Sarvian area.

303
304

305

**Fig. 5.** Mineral prospectivity map of the Sarvian area which confirmed by iron outcrops.

307

**Fig. 6.** Mineral prospectivity map of the Sarvian area which confirmed by check field of three target

areas.